NASA TECHNICAL NOTE

NASA TN D-6117

C.1

NASA TN D-6117

UTILIZATION OF A FIXED-BASE SIMULATOR TO STUDY THE STALL AND SPIN CHARACTERISTICS OF FIGHTER AIRPLANES

by Frederick L. Moore, Ernie L. Anglin, Mary S. Adams, Perry L. Deal, and Lee H. Person, Jr.

Langley Research Center
Hampton, Va. 23365

NATIONAL AERONAUTICS AND SPACE ADMINISTRATION • WASHINGTON, D. C. • MARCH 1971

1. Report No. NASA TN D-6117	2. Government Accession No.	3. Recipient's Catalog No.
4. Title and Subtitle UTILIZATION OF A FIXED-BASE SIMULATOR TO STUDY THE STALL AND SPIN CHARACTERISTICS OF FIGHTER AIRPLANES		5. Report Date March 1971
		6. Performing Organization Code
7. Author(s) Frederick L. Moore, Ernie L. Anglin, Mary S. Adams, Perry L. Deal, and Lee H. Person, Jr.		8. Performing Organization Report No. L-7420
9. Performing Organization Name and Address NASA Langley Research Center Hampton, Va. 23365		10. Work Unit No. 126-62-11-01
		11. Contract or Grant No.
		13. Type of Report and Period Covered Technical Note
12. Sponsoring Agency Name and Address National Aeronautics and Space Administration Washington, D.C. 20546		14. Sponsoring Agency Code
15. Supplementary Notes		

16. Abstract

An investigation was conducted to determine the feasibility of using a fixed-base simulator for studies of the stall and spin characteristics of fighter airplanes. The simulator equipment consisted of a fixed-base cockpit with limited physical cues, including a visual display containing a target airplane for a realistic tracking task. The project was conducted as a real-time digital simulation with six-degree-of-freedom nonlinear equations of motion in which aerodynamic input data for two representative fighter configurations were used. One configuration was included to document its stall characteristics, whereas the spin and recovery characteristics of the other configuration were studied. The results of the study indicated that the fixed-base simulation technique could be employed for studying the stall and spin characteristics of an airplane.

17. Key Words (Suggested by Author(s)) Simulation; Stall and spin	18. Distribution Statement Unclassified – Unlimited

19. Security Classif. (of this report) Unclassified	20. Security Classif. (of this page) Unclassified	21. No. of Pages 34	22. Price* $3.00

*For sale by the National Technical Information Service, Springfield, Virginia 22151

UTILIZATION OF A FIXED-BASE SIMULATOR TO STUDY THE STALL AND SPIN CHARACTERISTICS OF FIGHTER AIRPLANES

By Frederick L. Moore, Ernie L. Anglin, Mary S. Adams,
Perry L. Deal, and Lee H. Person, Jr.
Langley Research Center

SUMMARY

An investigation was conducted to determine the feasibility of using a fixed-base simulator for studies of the stall and spin characteristics of fighter airplanes. The simulator equipment consisted of a fixed-base cockpit with limited physical cues, including a visual display containing a target airplane for a realistic tracking task. The project was conducted as a real-time digital simulation with six-degree-of-freedom nonlinear equations of motion with aerodynamic input data based on wind-tunnel results. Two representative fighter configurations were studied. One configuration was included to document its stall characteristics, whereas the spin and recovery characteristics of the other configuration were studied.

The results of the study indicate that the fixed-base simulation technique proved to be sufficiently realistic to be useful for studies of stall and spin characteristics. In particular, the evaluation pilots reported that the visual display, buffet cues, tracking task, and limited acceleration cues (provided by an inflatable seat cushion and arm puller) provided stimuli that contributed to the representation of the stall and spin. It was possible to evaluate effects of airframe and stability-augmentation modifications on motions at the stall; and recovery techniques from the stall, incipient spin, and fully developed spin could also be evaluated. The results also indicated that the type of motions produced following the stall were very sensitive to the sequence and timing of the control inputs. In addition to its research value, the simulator offers promise as a procedures trainer for pilot training.

INTRODUCTION

Concern has recently arisen over the relatively poor stall and spin characteristics of contemporary fighter airplanes. Research and flight-test experience have shown that most of these airplanes have poor spin-recovery characteristics and that recovery from a fully developed spin on these airplanes can be difficult or impossible. The poor stall and spin characteristics of current fighter configurations should serve as adequate warning that consideration should be given to these characteristics during early design stages of future fighter airplanes; but the techniques available for such study are effective for only part of the problem, particularly because they do not put the pilot in the problem in any realistic sense. The test techniques presently available consist of (1) spin tests of dynamically scaled models in the Langley spin tunnel, (2) spin tests of radio-controlled free-flight models launched from a helicopter, and (3) analytical studies. These techniques provide a considerable amount of information regarding stall and spin characteristics, but they do not provide detailed information regarding airplane controllability at high angles of attack, nor do they provide information regarding the susceptability of the airplane to spins when in a tactical environment. The present report presents a technique which uses a piloted simulator in an attempt to provide this information. The technique uses a fixed-base simulator with limited physical cues and is conducted as a real-time digital simulation. The study consisted of an evaluation of the realism of the technique, and the results presented herein illustrate some typical applications of the technique.

SYMBOLS

Aerodynamic quantities are presented with respect to a body system of axes. Dimensional values herein are given in both the International System of Units (SI) and the U.S. Customary Units. Measurements and calculations were made in the U.S. Customary Units.

b	wing span, m (ft)
$\bar{c}$	mean aerodynamic chord, m (ft)
C_l	rolling-moment coefficient
C_m	pitching-moment coefficient
C_n	yawing-moment coefficient
C_X	longitudinal-force coefficient
C_Y	side-force coefficient
C_Z	vertical-force coefficient
g	acceleration due to gravity, 9.8 m/sec^2 (32.2 ft/sec^2)

I_X, I_Y, I_Z — moments of inertia about X, Y, and Z body axes, respectively, kg-m^2 (slug-ft^2)

I_{XZ} — product of inertia, kg-m^2 (slug-ft^2)

m — airplane mass, kg (slugs)

p,q,r — rolling, pitching, and yawing angular velocities, respectively, rad/sec

$\bar{q}$ — dynamic pressure, $\frac{1}{2}\rho V^2$, N/m^2 (lb/ft^2)

S — wing area, m^2 (ft^2)

T — thrust, N (lb)

t — time, sec

u,v,w — longitudinal, side, and vertical velocity components, respectively, m/sec (ft/sec)

V — resultant linear velocity, m/sec (ft/sec)

X,Y,Z — body axes

α — angle of attack, deg

β — angle of sideslip, deg

δ_a — aileron and spoiler deflection, positive when trailing edge of right aileron is down and when left spoiler is up (left stick input), deg

δ_h — horizontal-tail deflection, positive when trailing edge is down (forward stick input), deg

δ_r — rudder deflection, positive when trailing edge is left (left pedal input), deg

ρ — air density, kg/m^3 (slugs/ft^3)

ϕ angle of bank, deg

θ angle of pitch, deg

$$C_{l_p} = \frac{\partial C_l}{\partial \frac{pb}{2V}} \qquad C_{n_p} = \frac{\partial C_n}{\partial \frac{pb}{2V}} \qquad C_{Y_p} = \frac{\partial C_Y}{\partial \frac{pb}{2V}}$$

$$C_{l_r} = \frac{\partial C_l}{\partial \frac{rb}{2V}} \qquad C_{n_r} = \frac{\partial C_n}{\partial \frac{rb}{2V}} \qquad C_{Y_r} = \frac{\partial C_Y}{\partial \frac{rb}{2V}}$$

$$C_{l_{\delta_a}} = \frac{\partial C_l}{\partial \delta_a} \qquad C_{n_{\delta_a}} = \frac{\partial C_n}{\partial \delta_a} \qquad C_{Y_{\delta_a}} = \frac{\partial C_Y}{\partial \delta_a}$$

$$C_{l_{\delta_r}} = \frac{\partial C_l}{\partial \delta_r} \qquad C_{n_{\delta_r}} = \frac{\partial C_n}{\partial \delta_r} \qquad C_{Y_{\delta_r}} = \frac{\partial C_Y}{\partial \delta_r}$$

$$C_{m_q} = \frac{\partial C_m}{\partial \frac{q\bar{c}}{2V}} \qquad C_{X_\alpha} = \frac{\partial C_X}{\partial \alpha} \qquad C_{Z_\alpha} = \frac{\partial C_Z}{\partial \alpha}$$

$$C_{m_\alpha} = \frac{\partial C_m}{\partial \alpha} \qquad C_{X_{\delta_h}} = \frac{\partial C_X}{\partial \delta_h} \qquad C_{Z_{\delta_h}} = \frac{\partial C_Z}{\partial \delta_h}$$

$$C_{m_{\delta_h}} = \frac{\partial C_m}{\partial \delta_h}$$

A dot over a symbol indicates a derivative with respect to time.

DESCRIPTION OF SIMULATOR

The stall and spin simulation technique used a modified fixed-base cockpit and limited physical and visual cues in an attempt to provide a realistic representation of airplane flight motions during stalls and spins. An overall view of the simulator system is presented in figure 1. The fixed-base cockpit is enclosed within a 6.1-meter-diameter (20-foot) sphere. Buffet cues are provided by a seat shaker, normal-acceleration cues by an inflatable seat cushion, and aural cues by an engine-noise generator.

A limited visual scene is provided by a combination of an earth-sky projector and a terrain projector. The earth-sky projector consists of a light source within a program-controlled plexiglass sphere which results in a blue-sky and brown-earth display that is primarily used for large-angle peripheral cues. A more narrow terrain display is used to provide the pilot with a more detailed visual display including the yawing cues necessary for stall and spin studies. The terrain features are provided by a terrain model, which is projected by a three-axis television probe (roll, pitch, and yaw) onto the surface of the sphere in front of the pilot. An additional scene consisting of a controllable target airplane for simulated air combat is also included in the visual display.

All of the simulator equipment is controlled by a real-time digital-computer system. It should be noted that the equipment used in the technique consists of components of conventional simulator systems with slight modifications.

Cockpit and Associated Equipment

A photograph of the cockpit used in the investigation is shown in figure 2. A typical fighter cockpit and instrument display were used in conjunction with additional equipment which provided limited kinesthetic and aural cues. A schematic representation of the cockpit environment is shown in figure 3. The seat shaker consisted of an electromagnetic shaker which operated at a frequency of 14 hertz. The amplitude of the seat shaker was programed to represent either constant buffet intensity or increasing buffet intensity with increasing angle of attack after buffet onset. An engine-noise generator, consisting of taped recordings of turbojet engine noise, was programed to indicate the noises associated with normal operation (including afterburner operation) and compressor stall and flameout. An arm puller, consisting of a strap worn by the pilot on his left arm, was provided to restrict throttle movements during high g maneuvers. The cockpit instrumentation was typical of current fighter airplanes and included angle-of-attack and angle-of-sideslip indicators. In addition to these devices, the cockpit was equipped with a pressurized seat cushion which was inflated and deflated under program control to provide limited normal-acceleration cues.

Visual Display

The visual display consisted of a blue-sky and brown-earth display, a detailed terrain display, and a target airplane. The earth-sky projector consisted of a plexiglass ball with one blue hemisphere and the other brown, which projected the sky and earth horizon image. In addition to providing the pilot with a field of view of $\pm 170^{\circ}$ horizontally and 90° to -60° vertically, the projector presented the pilot with 360° visual-motion cues about the pitch and roll axes at rates up to approximately 1.75 rad/sec. Since the earth-sky projector did not present motion about the yaw axis, a terrain projector was used to display detailed terrain features for yawing cues. The terrain display used the features of the three-dimensional model illustrated in figures 1 and 4. A three-axis television probe was used to provide roll, yaw, and pitch cues relative to the terrain features. The field of view of the probe was 33°, and it had the capability of showing rolling and yawing cues of $\pm 360^{\circ}$ and pitching cues of 30° to -90°. The maximum angular rates of the probe were 2.9 rad/sec for yaw, 2.7 rad/sec for roll, and 1.4 rad/sec for pitch. The camera was held at a fixed position over the model display to represent an altitude of 7620 m (25 000 ft); altitude variations were not simulated visually. The image from the probe was projected onto the surface of the 6.1-meter-diameter (20-foot) sphere in front of the pilot. The projected image was approximately 1.83 m (6 ft) in diameter and the horizons of the terrain display and the earth-sky display coincided at all times unless either the maximum roll rate of earth-sky projector or the maximum pitch rate of television probe was exceeded.

Consideration of the intended use of the simulator involved two points regarding the visual display. The first point was that without an outside visual task to increase pilot workload, recoveries from stalls would likely be immediate and lead to optimistic predictions of stall characteristics. The second point was that perhaps the most effective application of the technique would be an evaluation of the susceptibility of fighter designs to spins during vigorous tactical maneuvers. As a result of these considerations, a maneuverable target airplane was added to the visual scene to simulate a tactical environment. The features of the target airplane were provided by a scale-model airplane. The attitudes of the model were varied by computer program control through a gimbal system. The model image was projected by a television system in such a manner as to overlap the terrain and earth-sky display. The calculated relative range between the target airplane and the attacker airplane was indicated to the pilot by movement of the television camera which varied the size of the projected model image. The target airplane could be flown by program control through prescribed maneuvers, or it could be flown manually by a second pilot. The manual flying of the target airplane was simplified by requiring that the sideslip angle be zero at all times. As a result, the target airplane could be flown manually with a two-axis control stick (pitch and roll).

Computer Program and Equipment

The stall and spin simulator used real-time digital simulation techniques and equipment. The main components of the system are a digital computer, a real-time clock, and associated input-output equipment. The computer program used for this technique required a field length of 70 000 octal to compile and execute.

The motions of the airplane to be evaluated were produced by the equations of motion given in appendix A. The equations included six degrees of freedom and were set up for the input of nonlinear aerodynamic data. (Some of the aerodynamic data were input as a function of α and β and some as a function of α only.) The simplified equations of motion used for the target airplane are presented in appendix B. The piloting task for the target airplane was lessened by requiring that sideslip be zero at all times. The mathematical representation of the target airplane was also simplified by using linearized aerodynamic characteristics.

Airplane Configurations

The stall and spin simulator was evaluated by an investigation of the characteristics of two contemporary fighter configurations. The first airplane, referred to herein as configuration A, was a twin-jet swept-wing fighter; while the other airplane, configuration B, was a variable-sweep fighter design. The mass and dimensional characteristics of the airplanes are given in table I; the simulator control characteristics are listed in table II; and the aerodynamic data, which include nonlinearities of the static aerodynamic characteristics, are listed in table III. As shown in table III, aerodynamic data for configuration A were not available for angles of attack greater than 45°; as a result, the study of this configuration was limited to the stall and incipient spin and did not include developed-spin characteristics. Aerodynamic data were available for configuration B for angles of attack up to 90°, and developed spins were studied for this airplane.

It should be noted that the mass characteristics listed in table I show that both configurations have the mass heavily concentrated in the fuselage $\left(I_X - I_Y \text{ negative}\right)$. As pointed out in reference 1, the recommended spin-recovery control technique for airplanes having negative values of $I_X - I_Y$ is as follows: the elevator is moved to full trailing edge up; the ailerons are moved to full deflection with the spin; and the rudder is moved to full deflection against the spin. This recommended recovery technique was used by the pilots during this study and should be kept in mind during the subsequent discussion of spin characteristics.

Engine flameout during the strenuous tactical maneuvers used was simulated by computer logic involving programed tables of altitude and Mach number. When a preselected boundary was exceeded, engine thrust was instantaneously reduced to zero and reignition was assumed to occur when the angle of attack was reduced to 10° or less.

The characteristics of the target airplane are given in table IV. During the course of the study, the target airplane was flown by either manual control or program control.

EVALUATION PROCEDURES

The results of the investigation were in the form of pilot comments and time-history recordings for the various maneuvers performed. The investigation was conducted in two phases. The first phase consisted of evaluation of the equipment, and the second phase consisted of evaluation of the use of the equipment for the study of stall and spin problems.

Phase I

In the phase I evaluation of the overall simulation technique and equipment, the evaluation procedure consisted of simply allowing the pilot to fly the simulator in any manner he desired. The results were in the form of pilot comments and opinions on the adequacy of the simulation equipment, the various "cue" devices, and the overall simulation technique.

Phase II

Phase II was conducted in two parts by using the two different analytical airplanes. The first part consisted of evaluation of the use of the simulation technique for studies in the stall region using configuration A; and the second part consisted of evaluation of the use of the equipment for investigation of the spin using configuration B.

In evaluation of the simulation technique in the stall region using configuration A, the pilot was required to perform accelerated as well as normal (1g) stalls. (The angle of attack for stall for configuration A was approximately 21°.)

The normal stalls were performed by reducing the throttle to idle and then attempting to climb at a rate of 914.4 m/min (3000 ft/min) while maintaining wings level. The accelerated stalls were 2g level flight turns made with the throttle at the initial trimmed condition.

In evaluation of the simulation technique for study of spins using configuration B, the pilot repeated the stall maneuvers, but was required to fly farther into the stall region to induce spin-entry conditions. (The angle of attack for stall for configuration B was approximately 33°.) An additional maneuver was also conducted in which the pilot was required to track the target airplane in order to provide a realistic task that would divert his attention from simply flying the simulator. Use of this tracking task allowed the evaluation of the simulation technique for studying the possibility of unintentional spin entries while performing high g maneuvers. By providing the pilot with a variety of conditions at the stall, the ensuing different entries and spins provide for a more comprehensive evaluation of the total stall and spin picture.

RESULTS AND DISCUSSION

The adequacy of using a fixed-base simulator for studying airplane characteristics and pilot techniques during stalls and spins was evaluated by means of pilot comments and opinions and time-history recordings of the simulated stall and tracking maneuvers. Three research pilots participated in the complete simulation study, and two military pilots, having recent flight experience with high-performance fighter airplanes, flew configuration A as part of the phase I evaluation.

Phase I

In phase I, the simulation technique and equipment were evaluated by all pilots. The overall opinion was that the simulation technique could contribute to the realism of representing the stall and spin characteristics of fighter airplanes and would be useful as a research tool. The pressurized g cushion for representing normal acceleration was found to be more realistic if the g cushion was deflated for positive g rather than inflated. The arm puller on the left arm of the pilot (throttle controller) was found to be a good cue device except during a simulated spin; when this occurred, the strap restrained the left arm and would not allow the pilot to use both hands in applying recovery controls. Therefore, the arm puller was not used during the spin phase of the investigation. The seat shaker was found to be a good device for simulating airplane buffet; particularly, when the amplitude of the seat shaker increased with increasing angle of attack after buffet onset. The pilots felt that this provided a better representative warning of an impending stall than constant buffet intensity.

When using the televised visual display, the pilots felt the yawing motions were easily detected and, in particular during unusual attitudes, the visual display was very good. The pilots commented that the visual cues appeared to be those of a hazy day with around 6.4 km (4 miles) visability. In simulating a spin, the visual display was said to be fairly good; however, the pilots commented that the main cue missing was the g loading experienced during a spin (lateral accelerations). The maneuvers of the target display were found to be more realistic when the target was flown manually rather than when it was preprogramed.

Phase II

The first part of the discussion of phase II deals with the stall characteristics of configuration A and the effects of airframe modifications on these characteristics. The second part of the discussion deals with the stall and spin characteristics of configuration B including studies of the developed spin. Only the three research pilots flew phase II.

Configuration A.- Since the major objective of this study was to develop a technique for studying the stall and spin characteristics of fighter airplanes, it was desirable to simulate an airplane with fairly well-known stall and spin characteristics. The initial phase of the study was therefore conducted with configuration A. A review of the aerodynamic and stall characteristics of this configuration is presented in reference 2. In general, the flying characteristics of this airplane are typical of most fighter configurations at high angles of attack. Among the more predominant characteristics exhibited by the airplane at high angles of attack are (1) a lightly damped lateral oscillation (termed "wing rock"), (2) large values of adverse yaw due to aileron deflection, (3) loss of aileron effectiveness as a means of roll control, and (4) loss of directional stability at the stall.

The time history for a typical 1g stall for configuration A for a condition having rate stability augmentation about all three axes is presented in figure 5. During this stall maneuver, an indication of flow separation was introduced by simulated buffet (seat shaker), which began at $\alpha = 10^{\circ}$. As the angle of attack was increased, the pilots noted a significant degradation in roll-control effectiveness and increasing values of adverse yaw due to roll-control inputs. In general, wing rock began at an angle of attack of about 18°. When the angle of attack was increased to the stall, a directional divergence was experienced and the airplane rolled 360° to the left. Recovery from the poststall gyration was effected by returning the stick and pedal to neutral positions. The airplane normally recovered from such stalls in a near-vertical dive. The flight motions represented by the simulator were found to be representative of those exhibited by the airplane during actual flight tests. (A sample time history of such flight motions for the actual airplane is presented in fig. 6.)

A part of the study was directed at an evaluation of the effects of the stability-augmentation system and airframe modifications on stall characteristics. The stall characteristics were found to be relatively unaffected by operation of the stability-augmentation system. This result was probably caused by the fact that most stability-augmentation systems are designed for operation at lower angles of attack where the aerodynamic control surfaces are more effective. One airframe modification that appears to have a beneficial effect on stall characteristics is the addition of leading-edge flaps which increase both the lateral directional stability and dihedral effect at the stall, as pointed out in reference 2. A series of simulated stalls were therefore conducted to evaluate these devices. None of the time histories from these tests are presented herein, but the flight motions at the stall with the leading-edge flaps deflected were docile and easily controlled. It was found that the addition of leading-edge flaps delayed the directional divergence, and, as a result, the airplane could be flown to a higher angle of attack before divergence occurred. In addition, when the divergence was encountered, the rate of divergence was much lower than that exhibited by the basic airplane (no leading-edge flaps). The leading-edge flaps did, however, reduce the level of static longitudinal stability which, in turn, deteriorated the overall flying qualities of the airplane.

The pilots noted that the flight motions encountered during accelerated stalls were very similar to those of normal stalls, and recovery from the stall could be effected by neutralizing controls.

Configuration B.- The results for configuration B of the developed-spin tests are presented in figures 7 to 10. A typical calculated spin (no pilot) for configuration B is illustrated in figure 7. The motions were produced by the computer program when control inputs were made to produce a spin to the right (stick back, right pedal input, and stick left). The ensuing spin was extremely oscillatory and involved large oscillations about all three body axes. Angle of attack varied between 40° and 85° and the rate of yaw was about 1 rad/sec (about 6 sec per turn). Ailerons and rudder were moved to antispin stick (right and left pedal input) at $t = 45$ sec. Recovery from the spin was rapid, requiring less than one turn.

The spin illustrated in figure 7 is presented as a typical example of the spins encountered with the simulator; however, it was found that with the piloted simulator, the control-input sequencing differed from flight to flight and these variations in control inputs produced variations in the ensuing spins. Slight differences in input timing produced spins that were flatter and faster than that presented in figure 7. The critical nature of control-input timing was also verified during recoveries from incipient spins. For example, during the initial phase of certain oscillatory incipient-spin conditions when forward movement of the control stick (positive δ_h) was applied, the airplane generally recovered. However, beyond the initial phase of the incipient spin, forward control movement for recovery was useless or detrimental to recovery.

An example of an accelerated stall and spin obtained during the simulator study for configuration B is presented in figure 8. At the stall, a directional divergence was encountered and the airplane rolled "over the top" of the turn. Controls were neutralized, but the vehicle entered a spin that was slightly faster and flatter than that shown in figure 7. Recovery controls were applied at $t = 25$ sec, but recovery was slow and required about 5 turns (normally, recovery within $2\frac{1}{4}$ turns is considered satisfactory, ref. 1). The pilots commented that the variations in flight motions and recovery characteristics added to the realism of the simulator and prevented exact duplication of the piloting task.

Shown in figure 9 is an example of an inadvertent spin that occurred during simulated air-to-air combat. The target airplane was performing a hard turn to the left when the pilot of configuration B inadvertently stalled the airplane and entered a right spin. Throughout the spin, the pilot repeatedly applied spin-recovery controls but failed to maintain the control for a sufficient time to allow recovery. This type of pilot reaction is common during inadvertent spins by pilots unfamilar with spin characteristics of these particular configurations.

One particular area of concern during spin recovery is the possibility of spin reversals. Reversals occurred several times during the study, and a typical example is illustrated in figure 10. These motions were produced from a normal 1g stall. At $t = 45$ sec, spin-recovery controls were applied and recovery was relatively rapid but recovery controls were maintained too long and the airplane then entered a left spin. Pilot comments indicate that perhaps the most difficult task following recovery was deciding when to neutralize controls and prevent spin reversals. However, it is pointed out that several factors known to aid the pilot in preventing spin reversals were not present during the simulation. Some of these factors are g loadings on the pilot and vestibular cues after the rate of yaw has stopped.

APPLICATIONS OF THE SIMULATION

Based on the preceding results, it appears that fixed-base simulators can be used for study of stall and spin characteristics of high-performance airplanes. It should be noted, however, that the validity of the results of such simulator studies will depend upon how well the aerodynamic inputs of the simulated airplane have been documented.

The areas of potential application of the simulation technique include research and pilot training. As a research tool, the simulator has the capability of duplicating a tactical environment in which the stall and spin susceptibility of fighter airplanes can be studied. Also, the effects of airframe modifications and stability-augmentation systems can be evaluated. These applications imply that the capability of air-to-air combat simulators should be extended to include the stall and spin region for a more accurate representation of flight characteristics and maneuver limitations.

In the area of pilot training, the simulator could provide a means of training pilots for spin prevention and recovery. In this manner, pilots could (1) become familiar with the unusual flight motions associated with spinning (in particular, oscillatory spins), (2) learn the relative merits of instrument and visual cues for spin recovery, (3) become familiar with proper control inputs for spin recovery, (4) experience the relatively slow recoveries of some aircraft, and (5) become familiar with the problem of spin reversal following recovery from a developed spin.

CONCLUDING REMARKS

Based on pilot comments and results obtained during an investigation to determine whether a fixed-base simulator could be used to study stall and spin characteristics of fighter airplanes, the following results have been obtained:

1. Techniques and equipment were developed which made the fixed-base simulation sufficiently realistic to be useful for studies of stall and spin characteristics.

2. Application of the simulation results is limited to airplanes whose aerodynamics have been thoroughly documented.

3. The visual display, buffet cues, tracking task, and limited acceleration cues that were provided by the inflatable seat cushion and arm puller proved to be important stimuli that contributed to the representation of the stall and spin.

4. Results showed that the simulation technique can determine significant effects of airframe modifications, alteration in the stability-augmentation system, and variation in pilot techniques.

5. In addition to its research value, the technique seems to offer promise as a procedures trainer for pilot training.

Langley Research Center,
National Aeronautics and Space Administration,
Hampton, Va., January 13, 1971.

APPENDIX A

EQUATIONS OF MOTION FOR ATTACK AIRPLANE

The equations of motion used to calculate the flight motions of the attack airplane (airplane under evaluation) for the present study were

Rolling moment:

$$\dot{p} = \frac{I_Y - I_Z}{I_X} qr + \frac{\rho V^2 Sb}{2I_X}\left(C_l + C_{l_{\delta_a}}\delta_a + C_{l_{\delta_r}}\delta_r\right) + \frac{\rho V S b^2}{4I_X}\left(C_{l_p} p + C_{l_r} r\right)$$

Pitching moment:

$$\dot{q} = \frac{I_Z - I_X}{I_Y} pr + \frac{\rho V^2 S\bar{c}}{I_Y}\left(C_m + C_{m_{\delta_h}}\delta_h\right) + \frac{\rho V S\bar{c}^2}{4I_Y} C_{m_q} q$$

Yawing moment:

$$\dot{r} = \frac{I_X - I_Y}{I_Z} pq + \frac{\rho V^2 Sb}{2I_Z}\left(C_n + C_{n_{\delta_a}}\delta_a + C_{n_{\delta_r}}\delta_r\right) + \frac{\rho V S b^2}{4I_Z}\left(C_{n_p} p + C_{n_r} r\right)$$

Longitudinal force:

$$\dot{u} = -g \sin \theta + vr - wq + \frac{\rho V^2 S}{2m}\left(C_X + C_{X_{\delta_h}}\delta_h\right) + \frac{T}{m}$$

Side force:

$$\dot{v} = g \cos \theta \sin \phi + wp - ur + \frac{\rho V^2 S}{2m}\left(C_Y + C_{Y_{\delta_a}}\delta_a + C_{Y_{\delta_r}}\delta_r\right) + \frac{\rho V S b}{4m}\left(C_{Y_p} p + C_{Y_r} r\right)$$

Vertical force:

$$\dot{w} = g \cos \theta \cos \phi + uq - vp + \frac{\rho V^2 S}{2m}\left(C_Z + C_{Z_{\delta_h}}\delta_h\right)$$

APPENDIX B

EQUATIONS OF MOTION FOR TARGET AIRPLANE

The simplified equations of motion used to calculate the flight motions of the target airplane were

Rolling moment:

$$\dot{p} = \frac{I_Y - I_Z}{I_X} qr + \frac{\rho V^2 Sb}{2I_X}\left(C_{l_{\delta_a}} \delta_a\right) + \frac{\rho V S b^2}{4I_X} C_{l_p} p$$

Pitching moment:

$$\dot{q} = \frac{I_Z - I_X}{I_Y} pr + \frac{\rho V^2 S\bar{c}}{2I_Y}\left(C_m + C_{m_{\delta_h}} \delta_h + C_{m_\alpha} \alpha\right) + \frac{\rho V S \bar{c}^2}{4I_Y} C_{m_q} q$$

Yawing velocity:

$$r = \frac{wp + g \cos \theta \sin \phi}{u}$$

Longitudinal force:

$$\dot{u} = -g \sin \theta + vr - wq + \frac{\rho V^2 S}{2m}\left(C_X + C_{X_{\delta_h}} \delta_h + C_{X_\alpha} \alpha\right) + \frac{T}{m}$$

Vertical force:

$$\dot{w} = g \cos \theta \cos \phi + uq - vp + \frac{\rho V^2 S}{2m}\left(C_Z + C_{Z_{\delta_h}} \delta_h + C_{Z_\alpha} \alpha\right)$$

The side-force equation was assumed satisfied at all times, so that $\dot{v} = 0$ and no sideslip was experienced by the target airplane.

REFERENCES

1. Neihouse, Anshal I.; Klinar, Walter J.; and Scher, Stanley H.: Status of Spin Research for Recent Airplane Designs. NASA TR R-57, 1960. (Supersedes NACA RM L57F12.)
2. Chambers, Joseph R.; and Anglin, Ernie L.: Analysis of Lateral-Directional Stability Characteristics of a Twin-Jet Fighter Airplane at High Angles of Attack. NASA TN D-5361, 1969.

TABLE I.- MASS AND DIMENSIONAL CHARACTERISTICS

Configuration A:	
Weight, N (lb)	160 967 (36 187)
Wing area, m^2 (ft^2)	49.24 (530.00)
Wing span, m (ft)	11.71 (38.41)
Mean aerodynamic chord, m (ft)	4.89 (16.042)
I_X, kg-m^2 (slug-ft^2)	35 397 (26 108)
I_Y, kg-m^2 (slug-ft^2)	157 574 (116 222)
I_Z, kg-m^2 (slug-ft^2)	178 457 (131 625)
I_{XZ}, kg-m^2 (slug-ft^2)	0 (0)
Maximum control-surface deflections:	
δ_h, deg	9, -21
δ_a, deg	±30
δ_r, deg	±15
Configuration B:	
Weight, N (lb)	222 410 (50 000)
Wing area, m^2 (ft^2)	48.77 (525.0)
Wing span, m (ft)	19.20 (63.0)
Mean aerodynamic chord, m (ft)	2.76 (9.04)
I_X, kg-m^2 (slug-ft^2)	67 790 (50 000)
I_Y, kg-m^2 (slug-ft^2)	427 348 (315 200)
I_Z, kg-m^2 (slug-ft^2)	476 564 (351 500)
I_{XZ}, kg-m^2 (slug-ft^2)	0 (0)
Maximum control-surface deflections:	
δ_h, deg	10, -25
δ_a, deg	±15
δ_r, deg	±30

TABLE II.- SIMULATOR CONTROL CHARACTERISTICS

Control	Maximum travel		Breakout forces		Force deflection	
	cm	in.	N	lb	N/cm	lb/in.
Configuration A						
Stick:						
Forward	9.04	3.56	4.45	1	7.01	4
Back	18.67	7.35	4.45	1	7.01	4
Roll	7.37	±2.90	8.90	2	7.01	4
Pedal	8.26	3.25	80.07	18	113.83	65
Configuration B						
Stick:						
Forward	9.91	3.9	4.45	1.0	12.26	7.0
Back	15.75	6.2	4.45	1.0	12.26	7.0
Roll	12.19	±4.8	4.45	1.0	12.26	7.0
Pedal	8.26	3.25	80.07	18	113.83	65

TABLE III.- AERODYNAMIC CHARACTERISTICS

(a) Configuration A

Basic configuration

β, deg → / α, deg ↓	C_Y 0	C_Y 5	C_Y 10	C_Y 20	C_Y 30	C_Y 40	C_n 0	C_n 5	C_n 10	C_n 20	C_n 30	C_n 40	C_l 0	C_l 5	C_l 10	C_l 20	C_l 30	C_l 40	C_X 0	C_Z 0	C_m 0
-20	0.0000	-0.0545	-0.1235	-0.2715	-0.3960	-0.5280	0.0000	0.0127	0.0315	0.0696	0.0904	0.0854	0.0000	-0.0031	-0.0055	-0.0087	-0.0072	-0.0063	-0.0090	1.1000	0.0450
-15														-0.0031	-0.0055	-0.0087	-0.0072	-0 0063	-0.0090	0 8000	0.0400
-10														-0.0035	-0.0063	-0.0100	-0.0081	-0.0072	-0.0102	0 5000	0.0150
-5														-0.0039	-0.0071	-0.0113	-0.0090	-0.0081	-0.0112	0.2000	-0.0100
0														-0.0043	-0.0079	-0.0126	-0.0042	-0.0090	-0.0124	-0.101	-0.0325
5			-0.1180	-0.2760		-0.5390		0.0117	0.0301	0.0710	0.0865	0.0918	-0.0080	-0.0087	-0.0173	-0.0286	-0.0226	-0.0289	0.0000	-0.385	-0.0515
10			-0.1215	-0.2835	-0.4012	-0.4930		0.0120	0.0332	0.0713	0.0837	0.0875	-0.0080	-0.0093	-0.0230	-0.0380	-0.0368	-0.0480	0.0099	-0.707	-0.0862
15		-0.0355	-0.1040	-0.2855	-0.4050	-0.4930	0.0030	0.0106	0.0279	0.0642	0.0688	0.0706	-0.0080	-0.0132	-0.0252	-0.0385	-0.0369	-0 0513	0.0174	-0 9690	-0.1230
20		-0.0320	-0.1040	-0.2320	-0.3575	-0.4330	0.0030	0.0049	0.0145	0.0293	0.0374	0.0473	0.0000	-0.0063	-0.0097	-0.0210	-0.0321	-0 0527	-0.0025	-1.1050	-0 1174
25		-0.0385	-0.0545	-0.1690	-0.2870	-0.3870	0.0030	-0.0127	-0.0265	-0.0113	0.0142	0.0445		0.0004	-0 0030	-0.0271	-0.0449	-0 0593	-0.0174	-1 1930	-0.1814
30		-0.0260	-0.0385	-0.1250	-0.2760	-0.4190	0.0000	-0.0159	-0.0311	-0.0445	-0.0004	0.0332		-0.0024	-0.0070	-0.0120	-0.0459	-0 0762	-0.0174	-1 3260	-0 2382
35		-0.0190	-0.0295	-0.0810	-0.2075	-0.3770		-0.0177	-0.0343	-0.0487	-0.0247	0.0169		-0.0052	-0.0116	-0.0227	-0.0556	-0.0840	-0.0124	-1.4410	-0.2882
40		-0.0190	-0.0260	-0.0510	-0.1445	-0.3420		-0.0156	-0.0258	-0.0463	-0.0410	0.0085		-0.0116	-0.0212	-0 0352	-0.0617	-0 0879	-0.0149	-1 5670	-0 2981
45		-0.0160	-0.0495	-0.0425	-0.0845	-0.2430		-0.0081	-0.0128	-0.0371	-0 0523	0 0099		-0 0132	-0 0215	-0 0439	-0 0700	-0 0937	-0.0099	-1 5770	-0 3221

Modified configuration (leading-edge flaps installed)

β, deg → / α, deg ↓	C_Y 0	C_Y 5	C_Y 10	C_Y 20	C_Y 30	C_Y 40	C_n 0	C_n 5	C_n 10	C_n 20	C_n 30	C_n 40	C_l 0	C_l 5	C_l 10	C_l 20	C_l 30	C_l 40	C_X 0	C_Z 0	C_m 0
-20	0.0000	-0.0626	-0.1318	-0.2902	-0.4486	-0.6070	0.0000	0.0139	0.0317	0.0701	0.1085	0.1469	0.0000	-0 0012	-0 0021	-0.0074	-0.0127	-0 0192	-0 0200	1 1000	0 0400
-15														-0 0012	-0 0021	-0.0074	-0.0127	-0 0192	-0 0250	0 8000	0 0200
-10														-0.0013	-0.0024	-0 0084	-0 0144	-0 0212	-0 0300	0 5000	0 0000
-5														-0.0014	-0.0027	-0 0094	-0.0161	-0 0232	-0 0325	0 2000	-0 0180
0														-0 0015	-0.0030	-0.0104	-0.0178	-0 0252	-0 0325	-0 0851	-0 0373
5		-0.0577	-0.1286	-0.2803	-0.4320	-0.5837		0.0129	0.0314	0.0631	0.0948	0.1265		-0.0074	-0.0149	-0.0232	-0.0314	-0.0397	-0 0048	-0 3898	-0 0560
10		-0.0527	-0.1253	-0.2703	-0.4153	-0.5603	0.0030	0.0119	0.0311	0.0561	0.0811	0.1061	-0.0080	-0.1033	-0.0267	-0.0359	-0 0451	-0 0543	0.0232	-0 6944	-0 0746
15		-0.0461	-0.1055	-0.2637	-0.4219	-0.5801	0.0030	0.0079	0.0231	0.0629	0.1027	0.1425	-0.0080	-0.0128	-0 0231	-0.0399	-0.0567	-0 0735	0 0604	-0 9826	-0 0932
20		-0.0494	-0.1055	-0.2703	-0.4351	-0.5999	0.0030	0.0079	0.0192	0.0482	0.0772	0.1062	-0.0080	-0.0106	-0.0203	-0.0371	-0.0539	-0 0707	0 0790	-1 2381	-0 1087
25		-0.0362	-0.0692	-0.1944	-0 3196	-0.4448	0.0000	0.0020	-0 0059	0.0403	0 0865	0.1327	0.0000	-0.0049	-0 0030	-0.0534	-0 1038	-0 1542	0 0325	-1 3232	-0 1398
30		-0 0296	-0.0426	-0.0890	-0 1352	-0.1814		-0.0126	-0.0311	-0.0455	-0.0599	-0.0743		-0 0054	-0.0102	-0 0242	-0 0382	-0 0522	0 0139	-1 4215	-0 1771
35		-0.0263	-0 0296	-0.0560	-0.0824	-0.1088		-0.0198	-0.0390	-0.0694	-0.0998	-0.1302		-0.0049	-0 0128	-0.0262	-0.0396	-0 0530	0 0185	-1 5067	-0 2330
40		-0.0198	-0.0263	0.0650	0.1563	0.2476		-0.0099	-0.0297	-0 0669	-0.1041	-0.1413		-0.0143	-0 0227	-0 0309	-0 0391	-0 0473	0 0139	-1 6246	-0 2951
45		-0.0198	-0.0263	0.0650	0.1563	0.2476		-0.0099	-0.0297	-0 0669	-0.1041	-0.1413		-0.0143	-0.0227	-0.0309	-0 0391	-0 0473	0 0139	-1 6246	-0 2951

Basic and modified configuration

α, deg	$C_{X_{\delta_h}}$, per deg	$C_{Z_{\delta_h}}$, per deg	$C_{m_{\delta_h}}$, per deg	C_{m_q}, per rad	$C_{Y_{\delta_r}}$, per deg	$C_{n_{\delta_r}}$, per deg	$C_{l_{\delta_r}}$, per deg	$C_{Y_{\delta_a}}$, per deg	$C_{n_{\delta_a}}$, per deg	$C_{l_{\delta_a}}$, per deg	C_{Y_p}, per rad	C_{n_p}, per rad	C_{l_p}, per rad	C_{Y_r}, per rad	C_{n_r}, per rad	C_{l_r}, per rad
-20	0.0007	-0.0065	-0.0100	-6.0000	0 0009	-0.0012	0.0004	0.0001	0.0000	-0.0004	0.0000	0 0000	-0 3030	1.4010	-0 6160	-0.0800
-15	0.0012	-0.0074			0.0009		0.0004			-0.0004			-0 2940		-0 6060	-0 0800
-10	0.0014	-0.0076			0.0010		0.0003			-0.0007			-0.2450		-0.6370	-0.0700
-5	0.0015	-0.0074			0.0020		0.0002			-0.0008			-0.2940		-0.6480	-0.0500
0	0.0017	-0.0101					0.0001			-0.0007			-0.2450		-0.6220	0.0160
5	0.0015	-0.0074	-0.0099				0.0002	0.0002	0.0001	-0.0008		-0.1000	-0.2940	1.1990	-0.6480	0.1130
10	0.0014	-0.0076	-0.0101			-0.0011	0.0002	0.0001	0.0001	-0.0007		-0.1000	-0.1640	1.1210	-0.4640	0.1870
15	0.0012	-0.0074	-0.0101	-6.0100		-0.0011	0.0002	-0.0001	0.0001	-0.0004	0.2460	-0.1500	-0.0340	1.1060	-0.2800	0 3050
20	0.0007	-0.0065	-0.0097	-6.1000	0.0017	-0.0009	0.0001	-0.0005	0.0002	-0.0004	0.1180	-0 2000	0.0100	0.8800	-0.2940	0.6160
25	0.0004	-0.0067	-0.0091	-6.8000	0.0010	-0.0006		-0.0003	0.0002	-0.0002	0.0300	-0.3000	-0.0340	0.3050	-0.4200	0.8830
30	-0.0002	-0.0067	-0.0064	-6.5700	0.0009	-0.0005		-0.0002	0.0003	-0.0002	0.5650	-0.2000	-0.0640	-0.7080	-0.2640	0.6380
35	-0.0008	-0.0049	-0.0060	-7.5700	0.0005	-0.0003		-0.0003	0.0001	-0.0001	0.0930	-0.0310	-0.0680	-0.6440	-0.1200	0 3850
40	-0.0011	-0.0050	-0.0035	-7.8000	0.0004	-0.0002		-0.0005	0.0002	-0.0001	-0.1030	-0.1150	-0.0440	-0.3440	0.0420	0.0720
45	-0.0011	-0.0049	-0.0012	-9.1100	0.0003	-0.0001		-0.0004	0.0001	-0.0001	-0.1380	-0 2000	-0.0460	-0.2210	-0.1320	0.0440

TABLE III.- AERODYNAMIC CHARACTERISTICS – Continued

(b) Configuration B

β, deg	C_Y									C_n								
α, deg	-40	-30	-20	-10	0	10	20	30	40	-40	-30	-20	-10	0	10	20	30	40
-10	0.547	0.436	0.324	0.145	0.000	-0.156	-0.320	-0.431	-0.542	-0.042	-0.042	-0.042	-0.020	0.000	0.016	0.036	0.036	0.036
-5	0.585	0.464	0.343	0.158		-0.143	-0.320	-0.441	-0.561	-0.042	-0.043	-0.044	-0.021		0.016	0.038	0.037	0.036
0	0.583	0.467	0.351	0.167		-0.126	-0.309	-0.425	-0.540	-0.039	-0.041	-0.042	-0.022		0.015	0.038	0.037	0.035
5	0.572	0.459	0.346	0.173		-0.106	-0.284	-0.397	-0.510	-0.037	-0.038	-0.039	-0.022		0.015	0.037	0.036	0.035
10	0.543	0.443	0.342	0.180		-0.102	-0.266	-0.367	-0.467	-0.035	-0.034	-0.034	-0.021		0.016	0.032	0.032	0.032
15	0.506	0.430	0.353	0.186		-0.097	-0.256	-0.339	-0.421	-0.029	-0.037	-0.024	-0.016		0.012	0.024	0.026	0.028
20	0.471	0.402	0.332	0.189		-0.084	-0.223	-0.297	-0.370	-0.005	-0.003	-0.001	-0.008		0.005	0.006	0.008	0.011
25	0.484	0.390	0.295	0.161		-0.051	-0.187	-0.282	-0.376	0.031	0.028	0.024	0.007		-0.006	-0.015	-0.010	-0.004
30	0.544	0.420	0.295	0.139		-0.017	-0.198	-0.323	-0.447	0.029	0.032	0.035	0.024		-0.021	-0.029	-0.020	-0.011
35	0.618	0.484	0.350	0.172		-0.042	-0.242	-0.377	-0.511	0.016	0.025	0.034	0.028		-0.027	-0.033	-0.025	-0.016
40	0.672	0.541	0.410	0.219		-0.097	-0.285	-0.416	-0.547	0.035	0.032	0.030	0.025		-0.021	-0.031	-0.033	-0.036
45	0.652	0.532	0.412	0.254		-0.126	-0.301	-0.422	-0.542	0.046	0.033	0.020	0.017		-0.013	-0.021	-0.034	-0.046
50	0.612	0.503	0.394	0.239		-0.127	-0.306	-0.416	-0.525	0.038	0.016	-0.005	-0.015		0.003	0.004	-0.017	-0.038
55	0.618	0.496	0.373	0.190		-0.097	-0.287	-0.410	-0.532	0.034	0.007	-0.020	-0.039		0.037	0.020	-0.007	-0.033
60	0.670	0.517	0.363	0.153		-0.051	-0.266	-0.424	-0.581	0.044	0.012	-0.020	-0.048		0.048	0.013	-0.018	-0.050
65	0.715	0.574	0.433	0.120		-0.049	-0.303	-0.444	-0.585	0.071	0.042	0.013	-0.049		0.038	-0.003	-0.032	-0.061
70	0.681	0.588	0.494	0.174		-0.075	-0.359	-0.453	-0.546	0.072	0.053	0.033	-0.023		0.021	-0.021	-0.040	-0.060
75	0.638	0.565	0.492	0.247		-0.107	-0.378	-0.451	-0.524	0.054	0.038	0.022	-0.008		0.006	-0.022	-0.038	-0.054
80	0.619	0.551	0.482	0.289		-0.143	-0.378	-0.447	-0.515	0.039	0.022	0.005	-0.012		-0.007	-0.013	-0.030	-0.047
85	0.615	0.546	0.476	0.310		-0.167	-0.370	-0.440	-0.509	0.037	0.016	-0.004	-0.014		-0.004	-0.006	-0.023	-0.040
90	0.620	0.546	0.471	0.317		-0.184	-0.355	-0.430	-0.504	0.027	0.009	-0.009	-0.015		0.008	0.002	-0.017	-0.033

β, deg	C_l									C_m								
α, deg	-40	-30	-20	-10	0	10	20	30	40	-40	-30	-20	-10	0	10	20	30	40
-10	-0.030	-0.017	-0.004	0.001	0.000	-0.004	0.004	0.017	0.030	0.119	0.155	0.191	0.269	0.329	0.291	0.248	0.184	0.1192
-5	-0.011	-0.003	0.006	0.003		-0.005	-0.007	-0.004	0.000	0.336	0.246	0.155	0.189	0.173	0.176	0.186	0.261	0.336
0	0.024	0.023	0.022	0.008		-0.012	-0.022	-0.024	-0.025	0.420	0.266	0.113	0.081	0.063	0.063	0.117	0.269	0.420
5	0.051	0.046	0.040	0.017		-0.021	-0.039	-0.045	-0.050	0.418	0.225	0.032	-0.031	-0.037	-0.050	0.026	0.222	0.418
10	0.076	0.060	0.044	0.020		-0.023	-0.046	-0.062	-0.078	0.418	0.160	-0.098	-0.142	-0.148	-0.162	-0.090	0.164	0.418
15	0.096	0.068	0.040	0.020		-0.024	-0.043	-0.071	-0.099	0.378	0.074	-0.229	-0.222	-0.218	-0.228	-0.215	0.081	0.378
20	0.096	0.065	0.033	0.019		-0.023	-0.038	-0.070	-0.101	0.326	0.013	-0.299	-0.307	-0.284	-0.309	-0.321	0.003	0.326
25	0.075	0.047	0.019	0.016		-0.019	-0.031	-0.059	-0.087	0.386	0.030	-0.326	-0.359	-0.401	-0.381	-0.361	0.013	0.386
30	0.065	0.039	0.012	0.007		-0.010	-0.015	-0.042	-0.068	0.491	0.083	-0.324	-0.343	-0.531	-0.437	-0.347	0.072	0.491
35	0.051	0.033	0.015	-0.006		0.000	-0.012	-0.030	-0.048	0.535	0.124	-0.287	-0.377	-0.579	-0.412	-0.337	0.099	0.535
40	0.038	0.023	0.008	-0.007		0.003	-0.017	-0.032	-0.047	0.486	0.121	-0.244	-0.493	-0.603	-0.439	-0.340	0.073	0.486
45	0.060	0.037	0.014	-0.005		-0.006	-0.023	-0.046	-0.069	0.247	0.037	-0.174	-0.115	-0.617	-0.550	-0.265	-0.009	0.247
50	0.091	0.065	0.038	0.002		-0.011	-0.030	-0.057	-0.083	0.073	-0.049	-0.170	-0.444	-0.626	-0.507	-0.091	-0.009	0.073
55	0.089	0.070	0.050	0.018		-0.019	-0.045	-0.065	-0.084	0.024	-0.113	-0.249	-0.515	-0.647	-0.410	-0.182	-0.079	0.024
60	0.087	0.070	0.052	0.028		-0.026	-0.051	-0.069	-0.086	-0.185	-0.299	-0.412	-0.638	-0.703	-0.482	-0.333	-0.259	-0.185
65	0.091	0.072	0.052	0.029		-0.028	-0.052	-0.070	-0.088	-0.494	-0.558	-0.621	-0.705	-0.805	-0.648	-0.470	-0.482	-0.494
70	0.092	0.072	0.052	0.027		-0.027	-0.053	-0.072	-0.090	-0.719	-0.773	-0.826	-0.868	-0.953	-0.812	-0.706	-0.713	-0.719
75	0.093	0.073	0.052	0.026		-0.016	-0.052	-0.073	-0.093	-0.868	-0.975	-1.082	-1.082	-1.136	-0.998	-0.999	-0.934	-0.868
80	0.095	0.072	0.049	0.027		0.000	-0.050	-0.073	-0.096	-1.000	-1.186	-1.371	-1.294	-1.328	-1.201	-1.308	-1.154	-1.000
85	0.095	0.072	0.049	0.029		-0.006	-0.061	-0.074	-0.097	-1.135	-1.351	-1.567	-1.541	-1.619	-1.493	-1.522	-1.329	-1.135
90	0.096	0.073	0.050	0.032		-0.027	-0.052	-0.075	-0.098	-1.274	-1.487	-1.700	-1.811	-1.974	-1.843	-1.672	-1.473	-1.274

TABLE III.- AERODYNAMIC CHARACTERISTICS – Concluded

(b) Configuration B – Concluded

α, deg	C_X	C_Z	$C_{X_{\delta_h}}$, per deg	$C_{Z_{\delta_h}}$, per deg	$C_{m_{\delta_h}}$, per deg	C_{m_q}, per rad	$C_{Y_{\delta_r}}$, per deg	$C_{n_{\delta_r}}$, per deg	$C_{l_{\delta_r}}$, per deg	$C_{Y_{\delta_a}}$, per deg	$C_{n_{\delta_a}}$, per deg	$C_{l_{\delta_a}}$, per deg	C_{Y_p}, per rad	C_{n_p}, per rad	C_{l_p}, per rad	C_{Y_r}, per rad	C_{n_r}, per rad	C_{l_r}, per rad
-10	-0.0090	0.8500	0.0061	-0.0127	-0.0264	-26.040	0.0035	-0.0014	0.0002	0.0005	-0.0002	-0.0008	0.030	-0.010	-0.140	0.120	-0.170	0.040
-5	-0.0250	0.4600	0.0055	-0.0156	-0.0297	-26.040	0.0034	-0.0013	0.0002	0.0005	-0.0002	-0.0008	0.060	-0.010	-0.190	0.130	-0.170	0.040
0	-0.0300	0.0800	0.0050	-0.0150	-0.0303	-26.040	0.0032	-0.0013	0.0002	0.0011	-0.0002	-0.0008	0.120	-0.010	-0.190	0.160	-0.170	0.040
5	-0.0286	-0.3200	0.0043	-0.0148	-0.0300	-24.420	0.0031	-0.0012	0.0002	0.0006	-0.0001	-0.0008	0.190	-0.010	-0.160	0.130	-0.170	0.090
10	0.0098	-0.7300	0.0035	-0.0143	-0.0305	-22.790	0.0029	-0.0013	0.0002	0.0006	-0.0001	-0.0009	0.230	-0.010	-0.180	0.010	-0.180	0.130
15	0.0451	-1.1300	0.0026	-0.0154	-0.0312	-26.230	0.0030	-0.0013	0.0001	0.0010	0.0000	-0.0008	0.240	0.000	-0.180	0.000	-0.220	0.220
20	0.0731	-1.5300	0.0017	-0.0184	-0.320	-29.670	0.0032	-0.0013	0.0001	0.0013	0.0001	-0.0008	0.230	0.010	-0.160	0.430	-0.260	0.310
25	0.0991	-1.9200	0.0008	-0.0207	-0.0344	-33.700	0.0033	-0.0013	0.0001	0.0018	0.0001	-0.0009	0.260	0.190	-0.180	1.050	-0.270	0.480
30	0.0920	-2.3300	-0.0003	-0.0241	-0.0370	-37.720	0.0032	-0.0013	0.0002	0.0014	0.0002	-0.0009	0.290	0.360	-0.260	1.200	-0.280	0.640
35	0.0708	-2.6500	-0.0012	-0.0250	-0.0361	-42.900	0.0029	-0.0012	0.0002	0.0013	0.0003	-0.0009	0.290	0.580	-0.380	0.790	-0.280	1.160
40	0.0465	-1.7470	-0.0021	-0.0220	-0.0316	-44.690	0.0025	-0.0009	0.0003	0.0027	0.0003	-0.0009	0.560	0.400	-0.550	0.230	-0.180	1.590
45	0.0397	-1.6896	-0.0035	-0.0169	-0.0247	-41.810	0.0019	-0.0007	0.0004	0.0014		-0.0009	1.230	0.260	-0.600	-0.180	-0.080	0.990
50	0.0354	-1.7054	-0.0043	-0.0144	-0.0174	-19.000	0.0019	-0.0006	0.0004	0.0007		-0.0007	1.700	0.190	-0.570	0.780	0.160	0.350
55	0.0392	-1.7492	-0.0048	-0.0120	-0.0114	2.000	0.0041	-0.0006	0.0003	0.0002		-0.0006	1.540	0.140	-0.450	2.610	0.990	0.250
60	0.0397	-1.7680	-0.0045	-0.0103	-0.0087	-7.000	0.0016		0.0001	-0.0013		-0.0005	-0.140	-0.310	-0.270	2.270	0.820	0.130
65	0.0344	-1.8142	-0.0047	-0.0093	-0.0034	-30.000	-0.0005		0.0001	-0.0035		-0.0005	-1.180	-0.470	-0.150	0.490	0.000	0.030
70	0.0358	-1.9020	-0.0052	-0.0105	-0.0040	-27.000	0.0004		0.0000	-0.0035		-0.0004	-0.090	-0.050	-0.100	-0.180	-0.110	0.000
75	0.0395	-1.9490	-0.0053	-0.0106	-0.0040	-4.000	0.0005		0.0000	-0.0027		-0.0005	0.640	-0.150	-0.100	-0.010	-0.110	0.010
80	0.0407	-1.9634	-0.0052	-0.0082	-0.0040	-3.000	-0.0000		0.0000	-0.0025		-0.0006	0.580	0.040	-0.133	0.090	-0.110	0.020
85	0.0412	-1.9690	-0.0056	-0.0071	-0.0040	-17.000	-0.0005		-0.0001	-0.0024		-0.0005	0.610	-0.040	-0.140	0.100	-0.110	0.010
90	0.0412	-1.9690	-0.0061	-0.0077	-0.0040	-24.000	-0.0008		-0.0002	-0.0024		-0.0002	0.730	-0.050	-0.150	0.160	-0.110	0.010

TABLE IV.- CHARACTERISTICS OF TARGET AIRPLANE

Mass and dimensional characteristics:	
Weight, N (lb)	160 967 (36 187)
Wing area, m^2 (ft^2)	50.01 (583.34)
Wing span, m (ft)	11.71 (38.41)
Mean aerodynamic chord, m (ft)	4.88 (16.00)
I_X, kg-m^2 (slug-ft^2)	35 397 (26 108)
I_Y, kg-m^2 (slug-ft^2)	157 574 (116 222)
I_Z, kg-m^2 (slug-ft^2)	178 457 (131 625)
I_{XZ}, kg-m^2 (slug-ft^2)	0 (0)
Aerodynamic data:	
C_X	-0.033
C_Z	-0.204
C_m	-0.000
C_{X_α}, per deg	0.002
C_{Z_α}, per deg	-0.060
C_{m_α}, per deg	-0.008
$C_{X_{\delta_h}}$, per deg	0.002
$C_{Z_{\delta_h}}$, per deg	-0.007
$C_{m_{\delta_h}}$, per deg	0.013
C_{m_q}, per rad	-6.000
C_{l_p}, per rad	-0.400
C_{n_r}, per rad	-0.400
$C_{l_{\delta_a}}$, per deg	-0.001

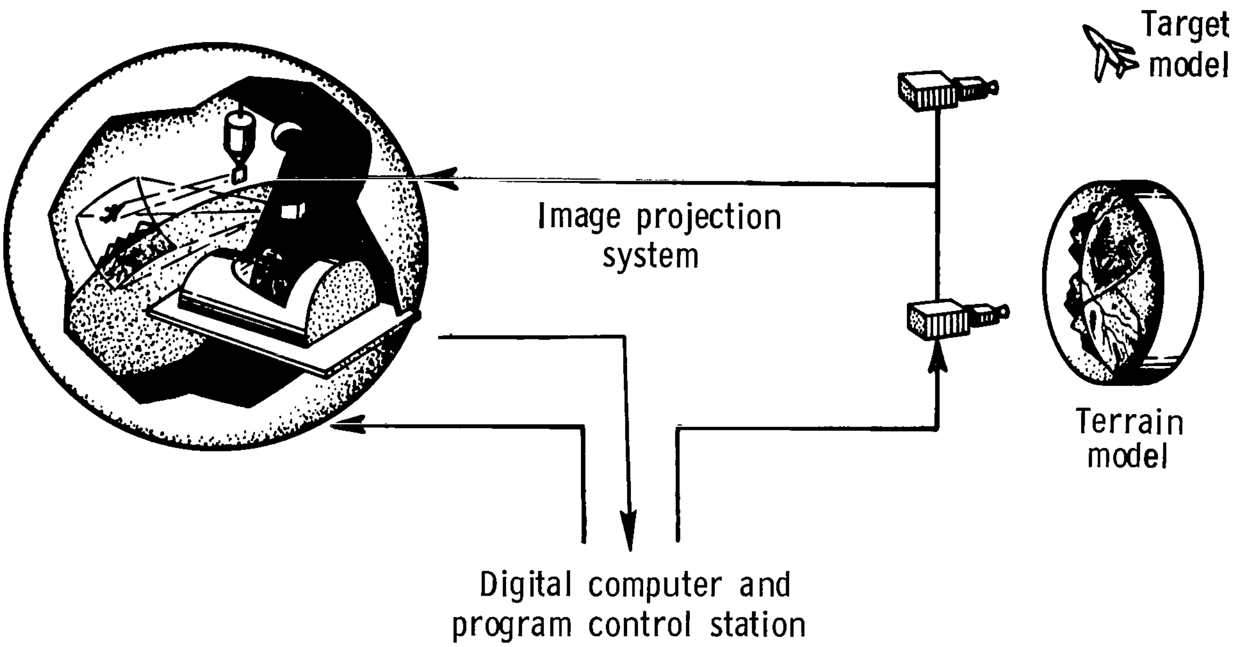

Figure 1.- Sketch of stall and spin simulation system.

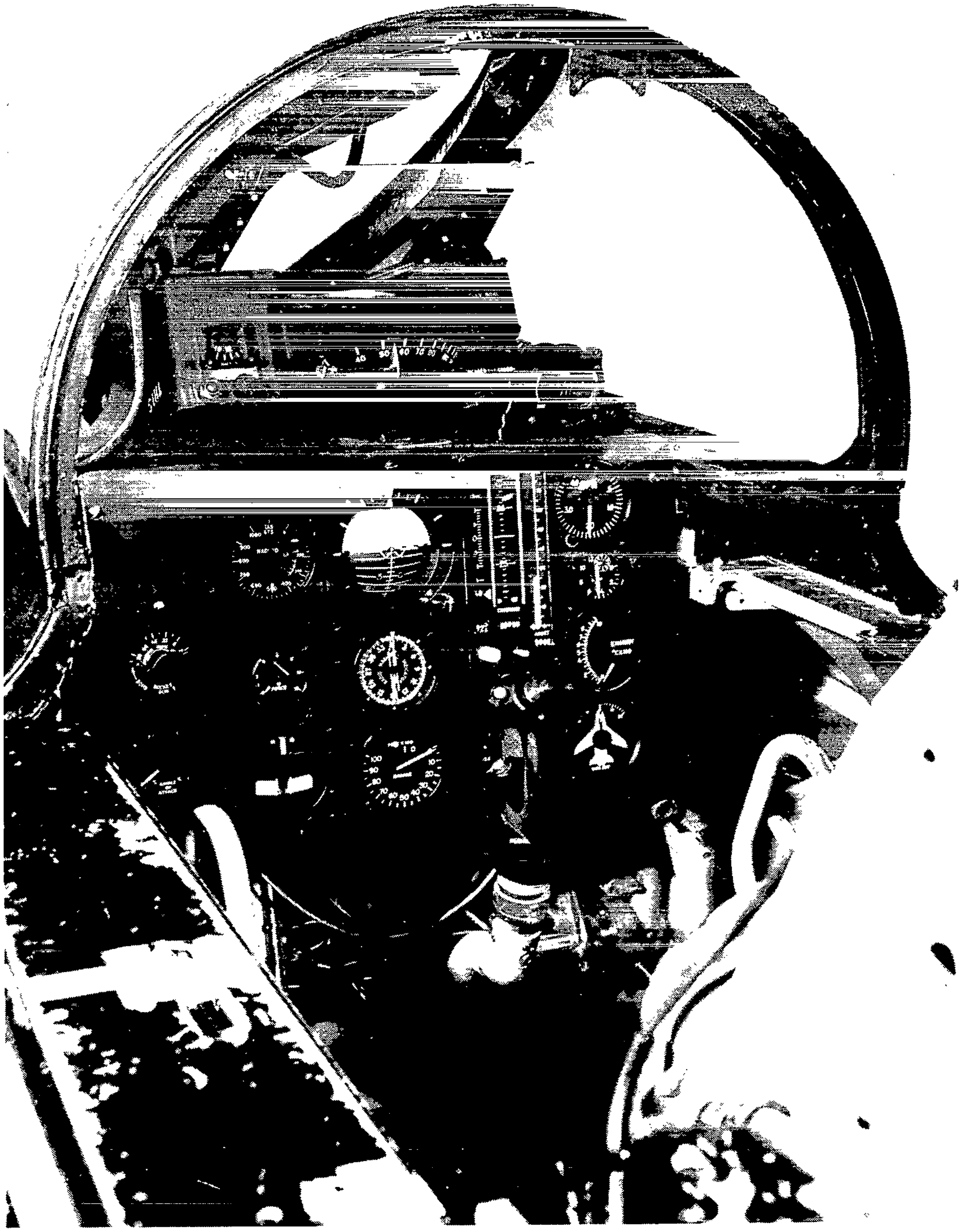

L-70-5520

Figure 2.- Photograph of cockpit.

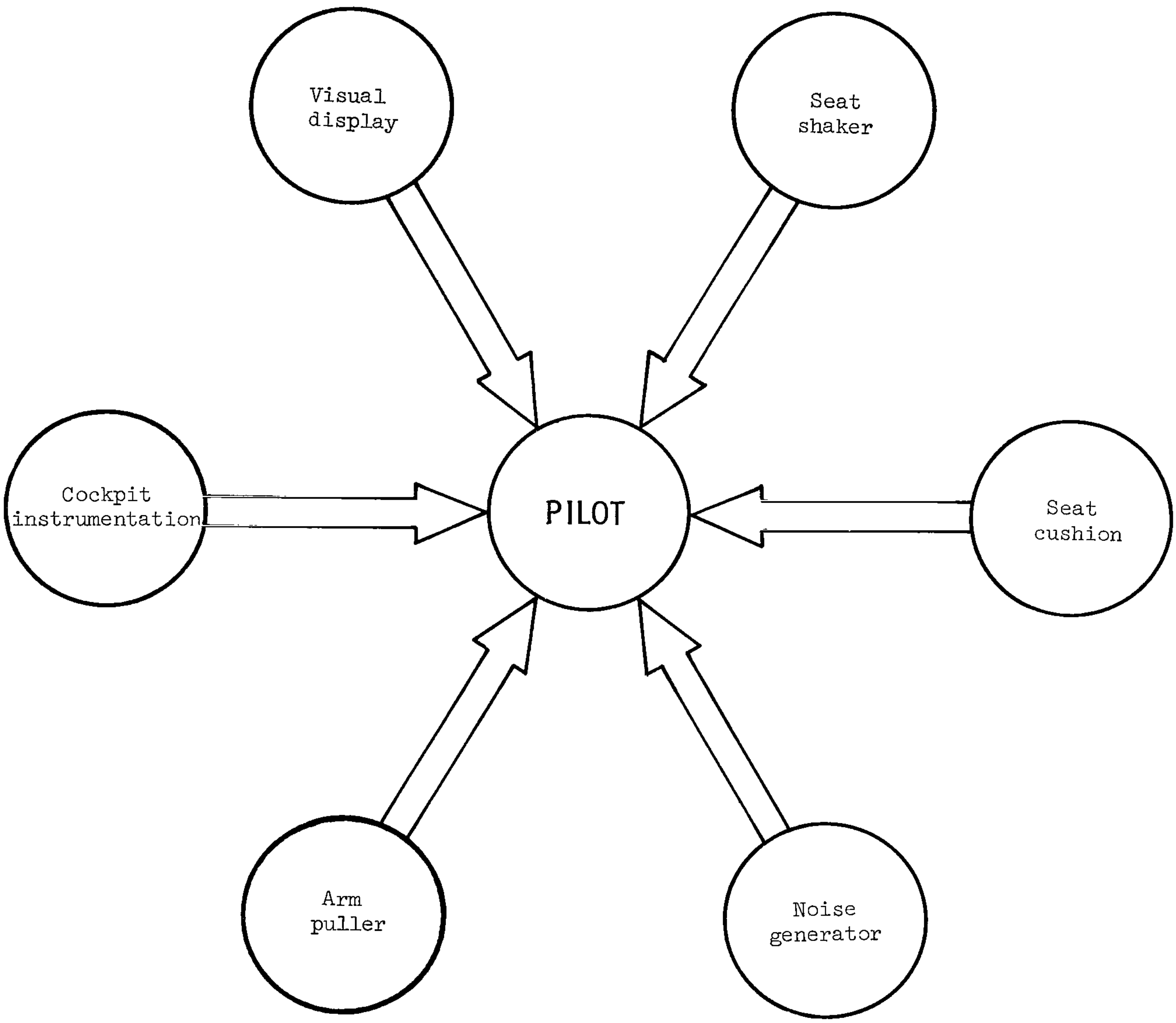

Figure 3.- Schematic of cockpit environment.

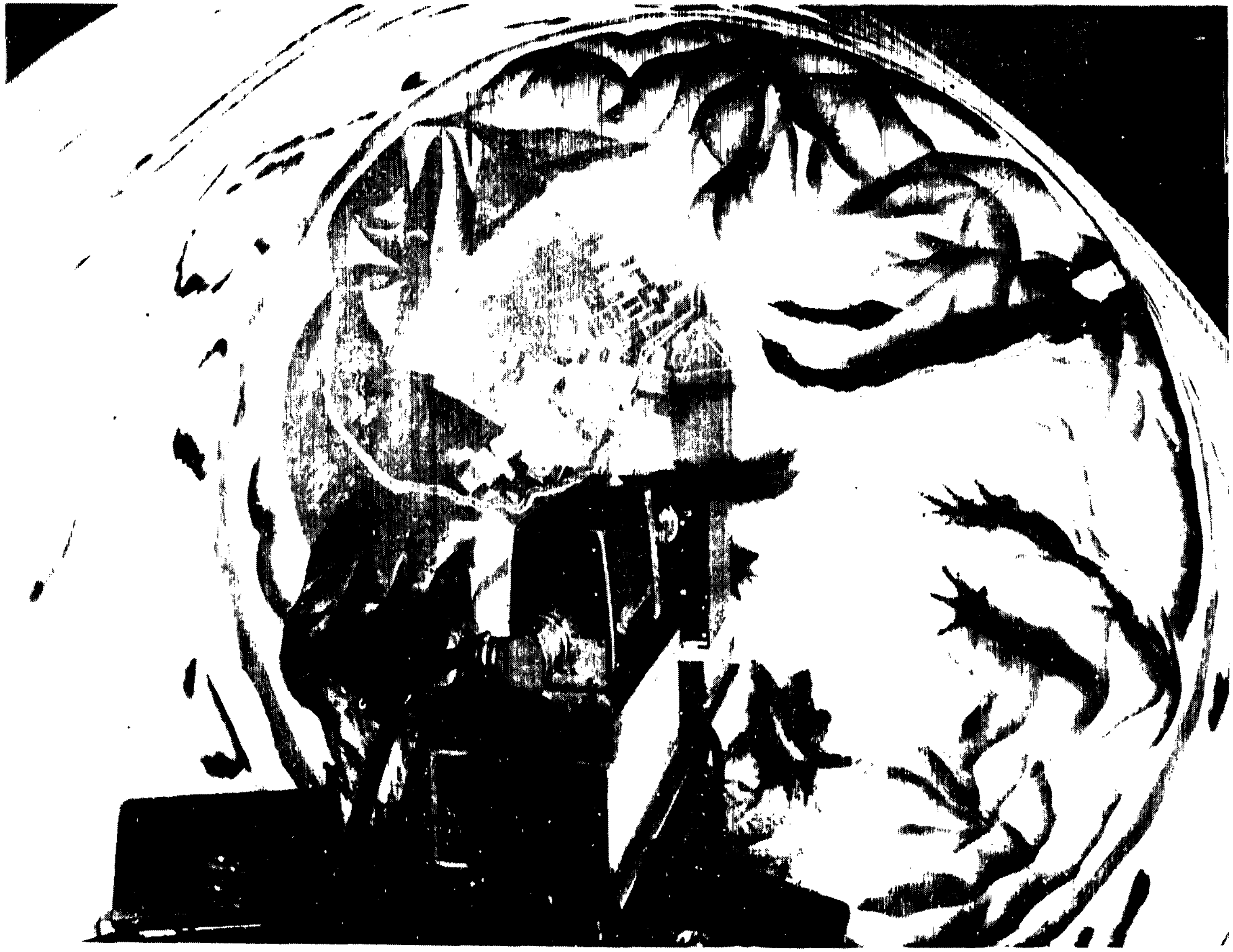

L-69-6689

Figure 4.- Photograph of terrain model.

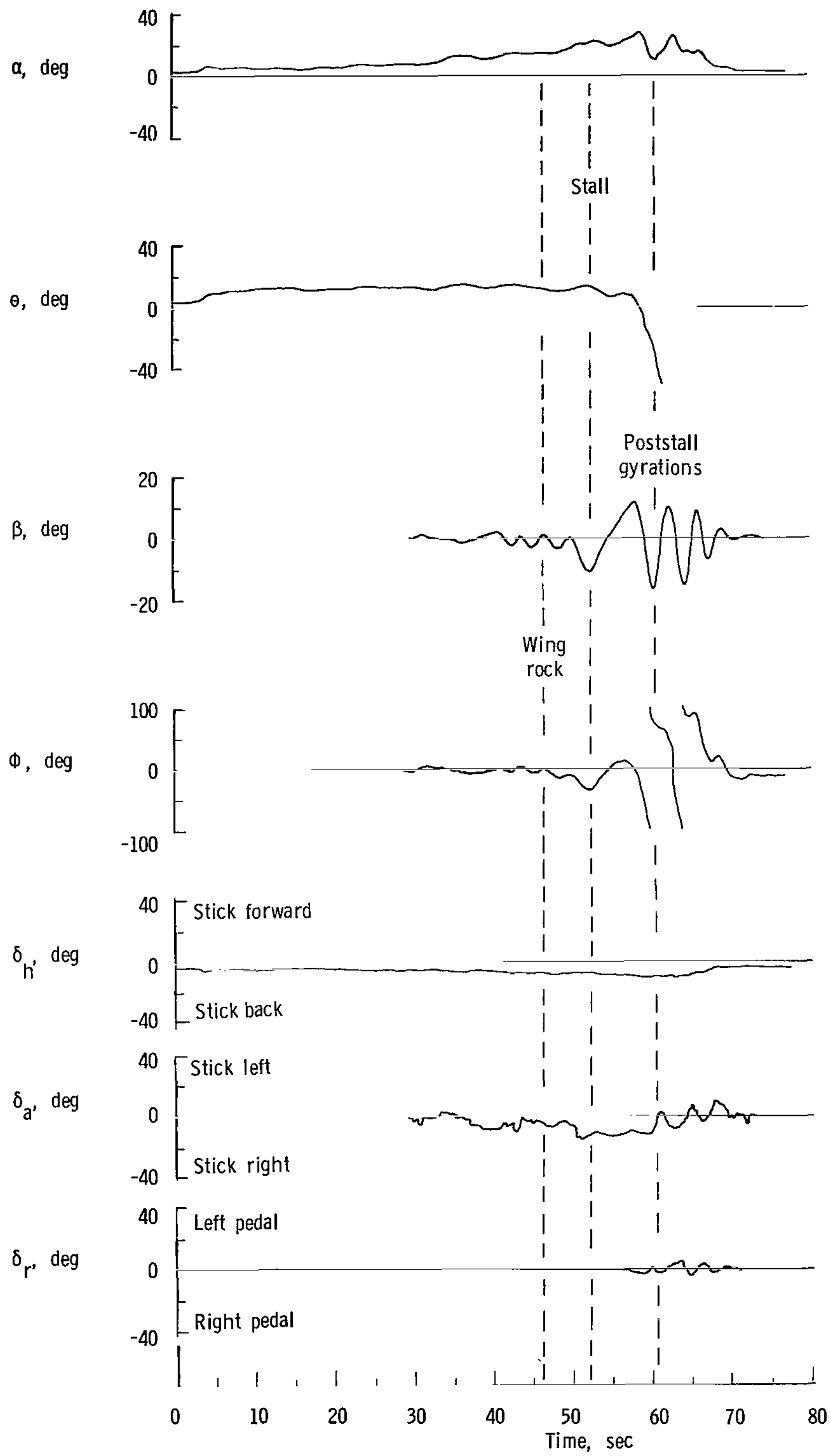

Figure 5.- Time history of a simulated 1g stall for configuration A with rate stability augmentation.

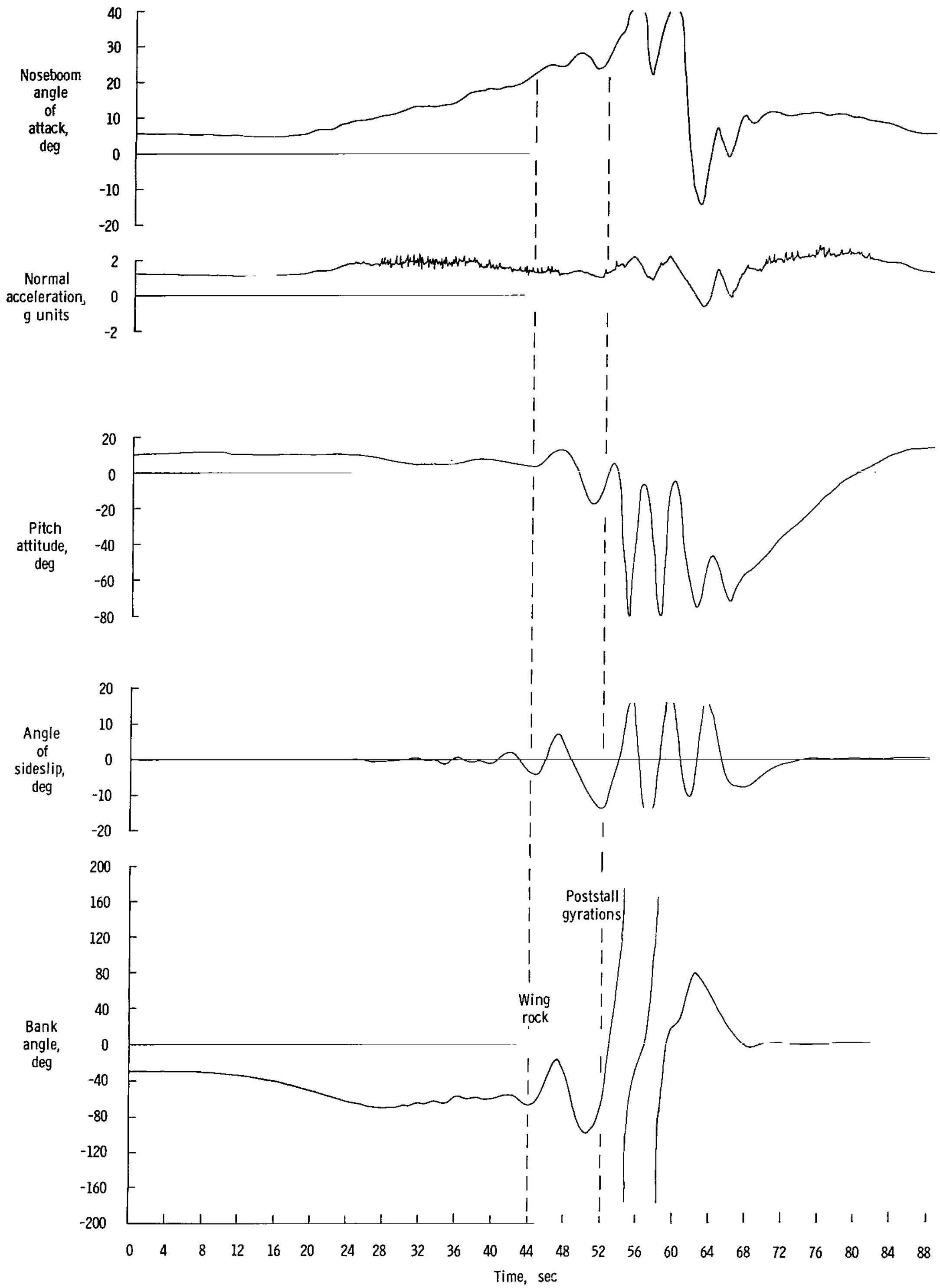

(a) Flight variables.

Figure 6.- Time histories of directional divergence encountered in actual flight.

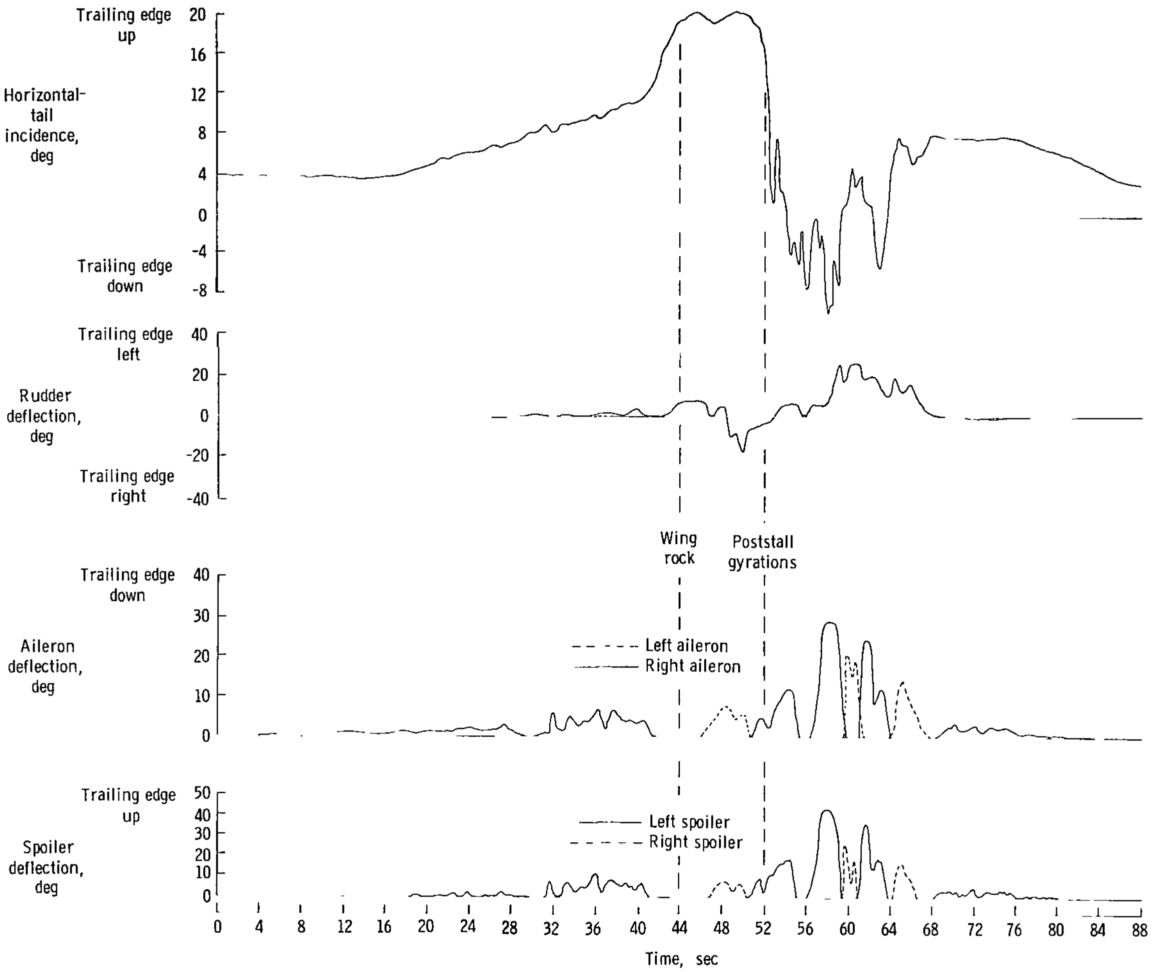

(b) Control-surface deflections.

Figure 6.- Concluded.

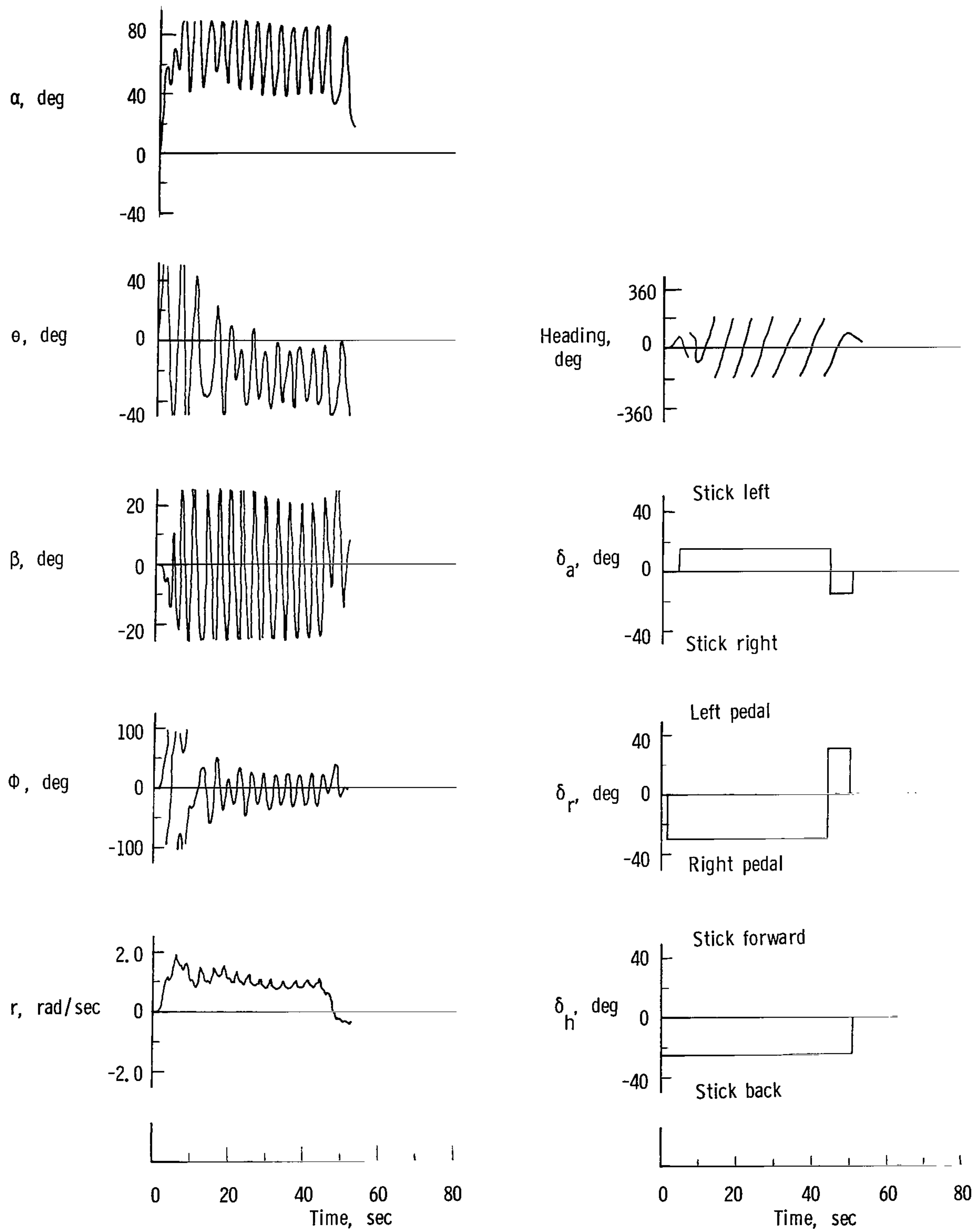

Figure 7.- Calculated spin for configuration B.

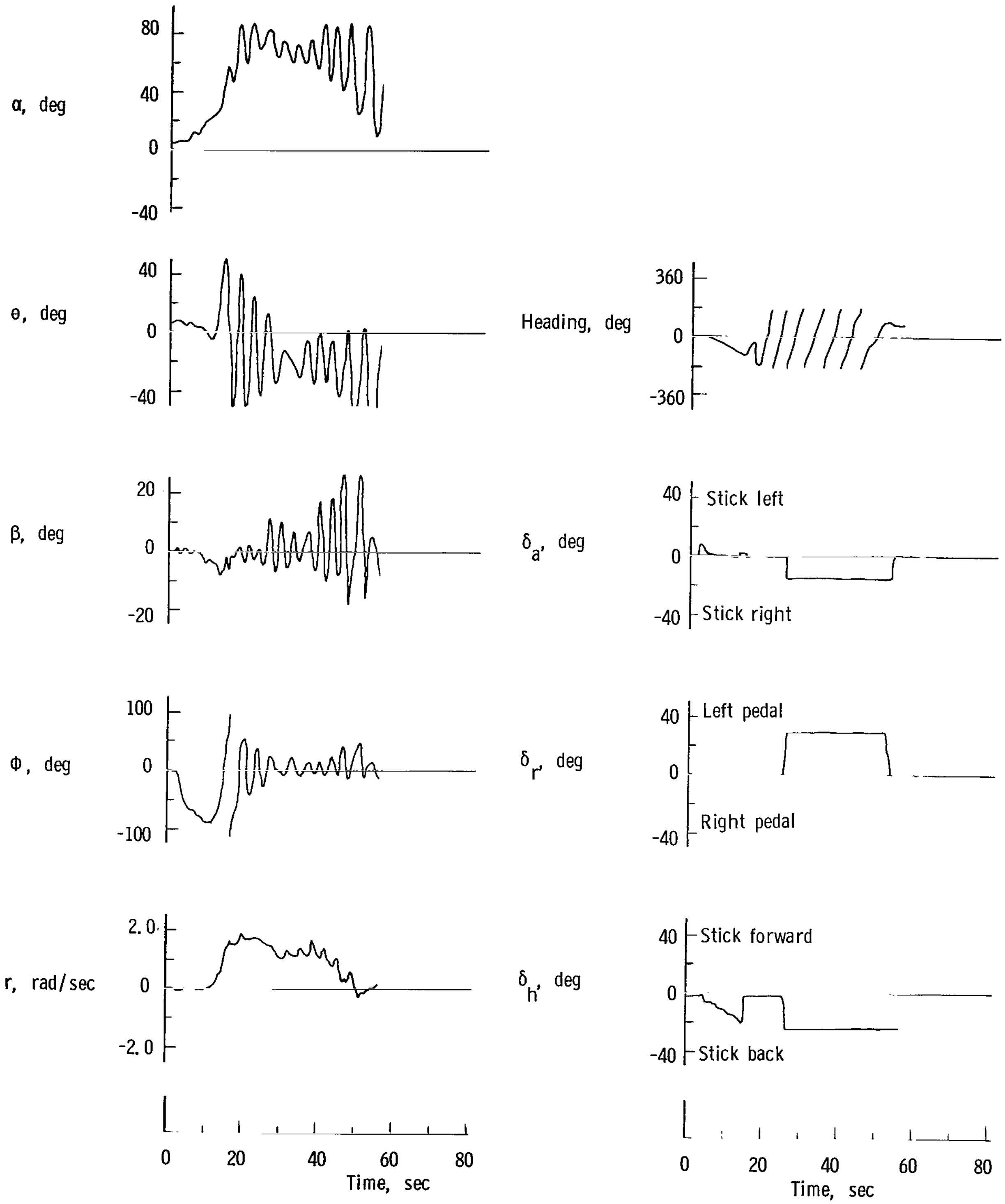

Figure 8.- Simulated accelerated stall and spin for configuration B.

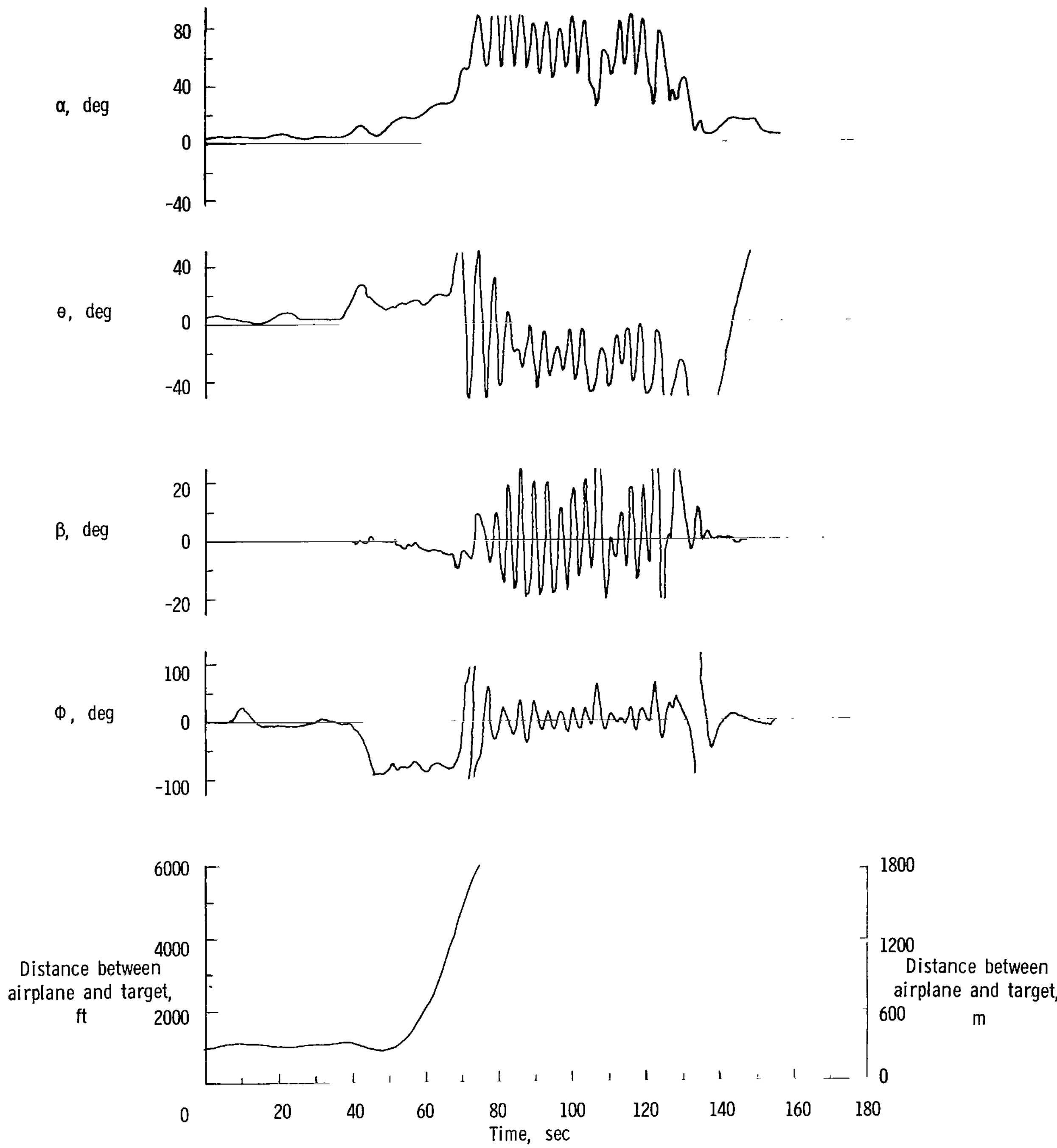

Figure 9.- Time history of inadvertent spin encountered during air-to-air combat simulation for configuration B.

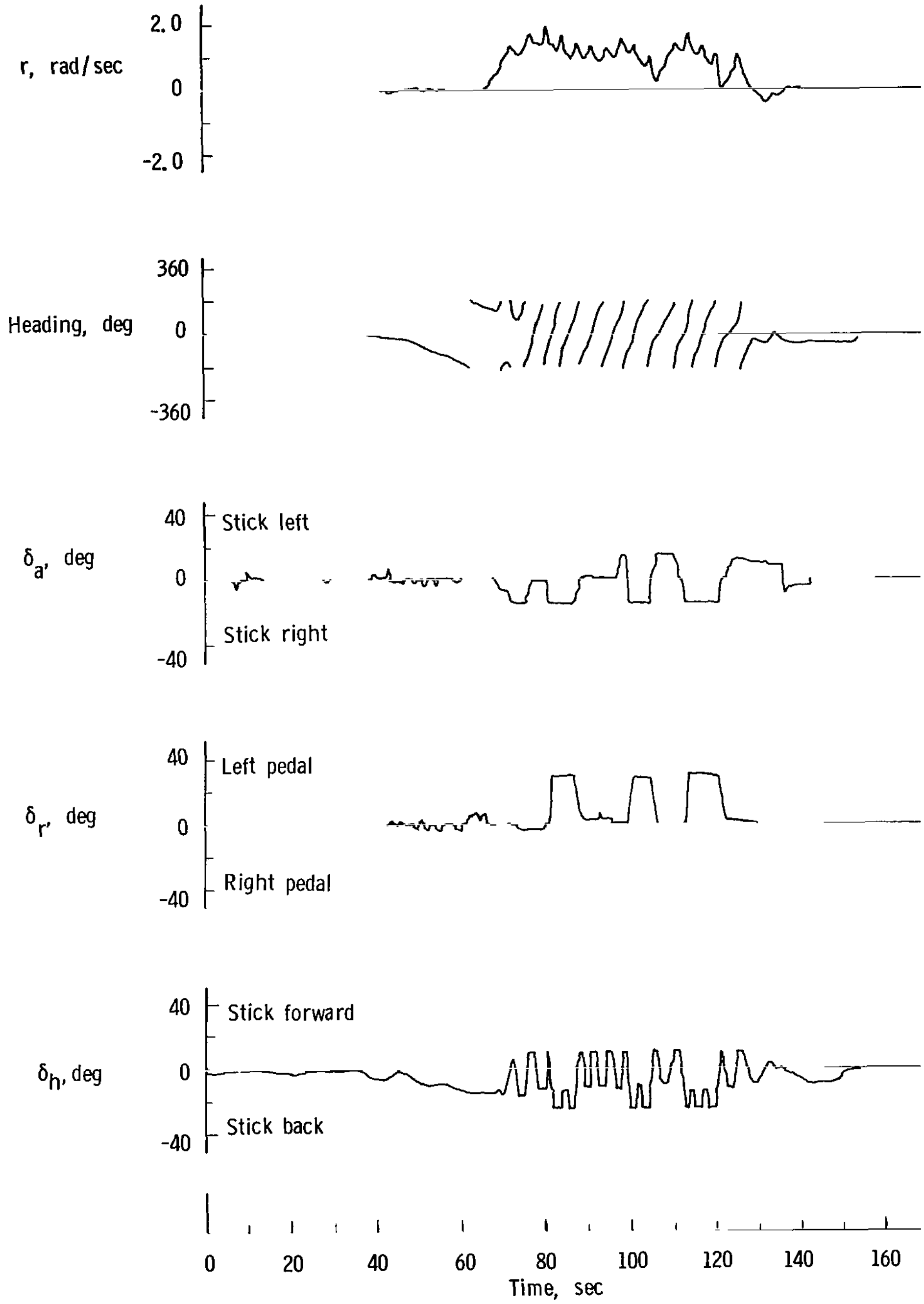

Figure 9.- Concluded.

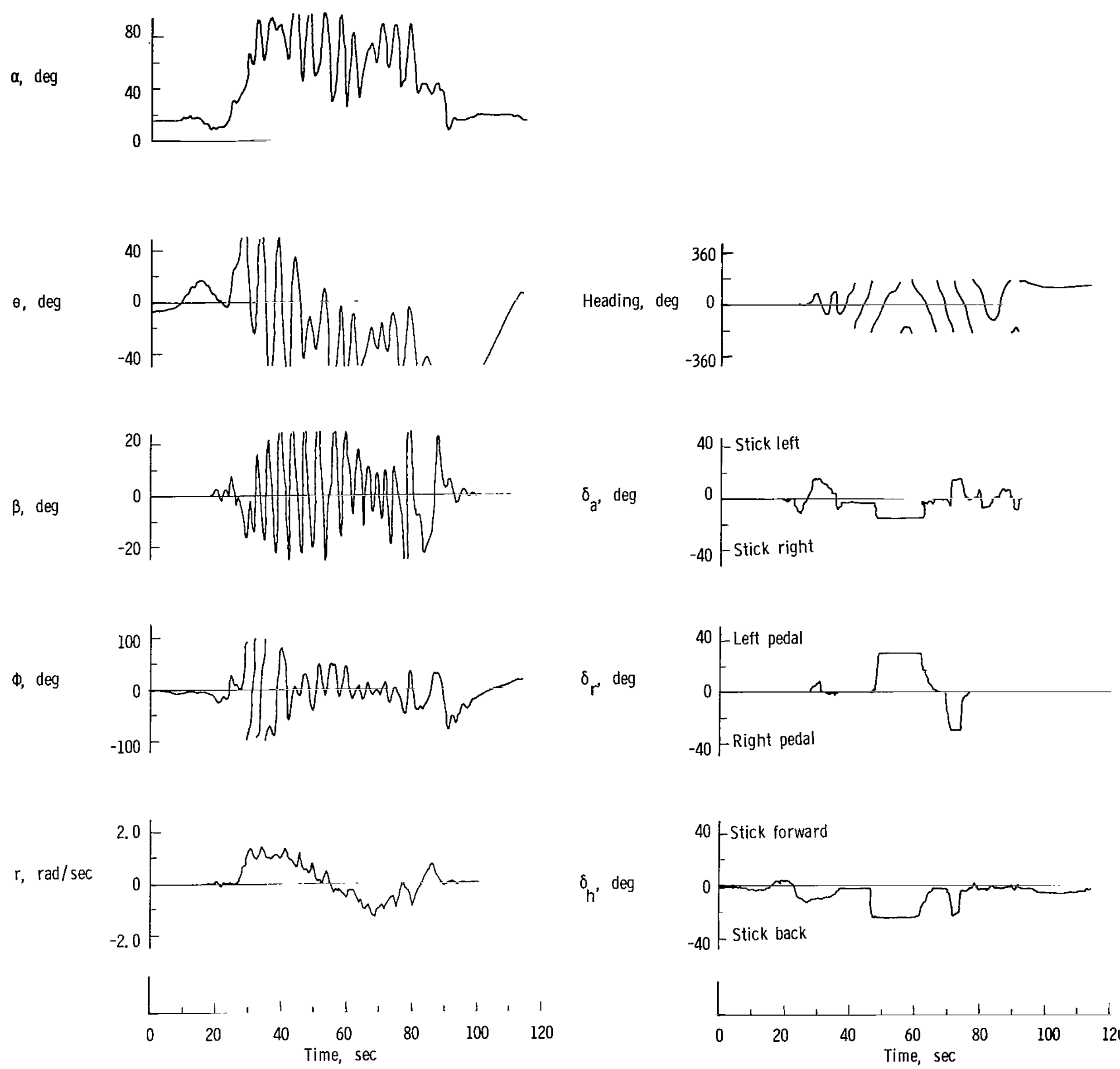

Figure 10.- Example of spin reversal for configuration B.

NASA-Langley, 1971 — 2 L-7420

NATIONAL AERONAUTICS AND SPACE ADMINISTRATION
WASHINGTON, D. C. 20546

OFFICIAL BUSINESS

FIRST CLASS MAIL

POSTAGE AND FEES PAID
NATIONAL AERONAUTICS AN
SPACE ADMINISTRATION

06U 001 27 51 3DS 71043 00903
AIR FORCE WEAPONS LABORATORY /WLOL/
KIRTLAND AFB, NEW MEXICO 87117

ATT E. LOU BOWMAN, CHIEF,TECH. LIBRARY

POSTMASTER: If Undeliverable (Section 158 Postal Manual) Do Not Retur

"The aeronautical and space activities of the United States shall be conducted so as to contribute . . . to the expansion of human knowledge of phenomena in the atmosphere and space. The Administration shall provide for the widest practicable and appropriate dissemination of information concerning its activities and the results thereof."

—NATIONAL AERONAUTICS AND SPACE ACT OF 1958

NASA SCIENTIFIC AND TECHNICAL PUBLICATIONS

TECHNICAL REPORTS: Scientific and technical information considered important, complete, and a lasting contribution to existing knowledge.

TECHNICAL NOTES: Information less broad in scope but nevertheless of importance as a contribution to existing knowledge.

TECHNICAL MEMORANDUMS: Information receiving limited distribution because of preliminary data, security classification, or other reasons.

CONTRACTOR REPORTS: Scientific and technical information generated under a NASA contract or grant and considered an important contribution to existing knowledge.

TECHNICAL TRANSLATIONS: Information published in a foreign language considered to merit NASA distribution in English.

SPECIAL PUBLICATIONS: Information derived from or of value to NASA activities. Publications include conference proceedings, monographs, data compilations, handbooks, sourcebooks, and special bibliographies.

TECHNOLOGY UTILIZATION PUBLICATIONS: Information on technology used by NASA that may be of particular interest in commercial and other non-aerospace applications. Publications include Tech Briefs, Technology Utilization Reports and Technology Surveys.

Details on the availability of these publications may be obtained from:

SCIENTIFIC AND TECHNICAL INFORMATION OFFICE

NATIONAL AERONAUTICS AND SPACE ADMINISTRATION

Washington, D.C. 20546